ELECTRON BEAM LONGITUDINAL DIAGNOSTIC WITH SUB-FEMTOSECOND RESOLUTION

G. Andonian[1], M. Harrison, F. O'Shea, A. Ovodenko, RadiaBeam Technologies, Santa Monica, CA, USA
M. Fedurin, K. Kusche, I. Pogorelsky, M. Polyanski,
C. Swinson, Brookhaven National Laboratory, Upton, NY, USA
M. Weikum, DESY, Hamburg, Germany
J. Duris, J. Rosenzweig, N. Sudar, UCLA, Los Angeles, CA, 90095
[1] also at UCLA, Los Angeles, CA 90095

Abstract

In this paper, we describe the status of prototype development on a diagnostic for high brightness electron beams, that has the potential to achieve sub-femtosecond longitudinal resolution. The diagnostic employs a high-power laser-electron beam interaction in an undulator magnetic field, in tandem with a rf bunch deflecting cavity to impose an angular-longitudinal coordinate correlation on the bunch which is resolvable with standard optical systems. The fundamental underlying angular modulation that is the basis of this diagnostic has been tested experimentally at the Brookhaven National Laboratory Accelerator Test Facility (BNL ATF) with a high-brightness electron beam and >100GW IR laser operating in the TEM_{10} mode. Here we provide an update on the status of the experimental program with details on the undulator testing, and initial results that include a study of the effects of the laser mode, and energy, on the beam angular projection.

INTRODUCTION

The precise characterization of the longitudinal profile of high-brightness electron beams is crucial for applications in light source development and advanced accelerator applications. Current techniques to measure the beam bunch profile include rf zero phasing methods, pulse reconstruction using interferometry of beam-based coherent radiation [1], and transverse deflecting cavities [2]. Deflecting cavities are very attractive because the presently attainable resolution with modern cavities in the x-band is on the order of a few fs. This paper describes a method to further enhance the resolution of the transverse deflecting cavity with the addition of an orthogonal transverse angular modulation on the beam correlated to the longitudinal coordinate. The correlation is generated by an interaction of the electron beam with a high-power laser in a resonant undulator. The interaction, similar to a higher-order inverse free-electron laser interaction, provides a correlated angular modulation that is resolvable on a distant screen with standard diagnostics and is schematically pictured in Fig. 1.

The interaction of the TEM_{10} laser mode, operating at high power and an electron beam in an undulator field yields an angular modulation on the beam. The detailed physical description is presented in Ref. [3]. For the system sketched in Fig. 1, the total angular modulation $\Delta x'$ is a function of

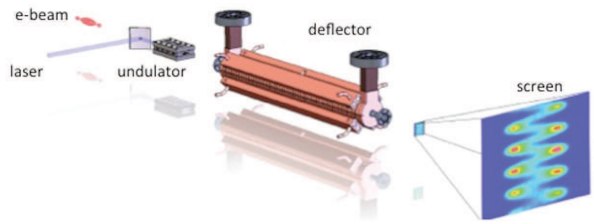

Figure 1: The electron beam interacts with a high-power, IR laser in the TEM_{10} mode, in a resonant undulator to provide a "fast", sinusoidal transverse angular modulation. The deflecting cavity provides a "slow" streak in the orthogonal dimension. The resultant combined downstream pattern yields information on the bunch profile with enhanced longitudinal resolution.

the longitudinal coordinate, s, and is given by the expression [4],

$$\Delta x' = Ak\sin(ks + \phi) \tag{1}$$

where k is the wavenumber of the driving laser, ϕ is the relative phase, and the amplitude of the oscillation, A, is proportional to

$$A \sim \frac{2K}{\gamma^2}\sqrt{\frac{P_L}{P_0}}[JJ] \tag{2}$$

In the expression for the amplitude A, K is the scaled undulator parameter, γ is the beam Lorentz factor, P_L is the laser power, and the coupling factor $[JJ] = J_0(K^2/(4+2K^2)) - J_1(K^2/4+2K^2))$. For application as a bunch length diagnostic, it is important to maximize this amplitude because the angular modulation projection on a downstream profile monitor is the direct observable. From the expression above, it is clear the oscillation amplitude scales as the $\sqrt{P_L}$ and inversely with γ^2. Therefore the interaction favors high power, long wavelength lasers, and low-moderate energy beams. Based on this scaling, an experiment was designed for the Brookhaven National Laboratory Accelerator Test Facility (BNL ATF). The BNL ATF has a long history in experiments based on laser-electron beam interactions due to the availability of a high-brightness beam and high-power, CO_2 based IR laser. The expected interaction based on relevant BNL ATF parameters for the electron beam (ϵ_n=1mm-mrad, E=48MeV, Q=300 nC) and high power laser operations ($\lambda = 10.6\mu m$, P_L= 100GW) is shown in Fig. 2 using

ISBN 978-3-95450-177-9

a resonant undulator (described in the next section) and a x-band rf defelecting cavity [5] (f=11.6 GHz, V_0=8MV). Results of Elegant [6] simulations for the BNL ATF parameters are shown below.

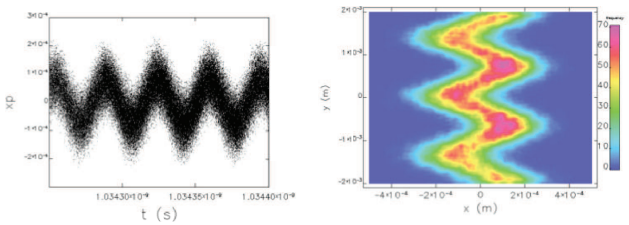

Figure 2: Simulations of angular beam modulation versus longitudinal coordinate after interaction in undulator (left) and transverse profile on diagnostic imaging screen 1m downstream.

UNDULATOR DEVELOPMENT

The design undulator parameter was K=2.49 with a period of 4cm to satisfy the resonant wavelength (10.6μm for the BNL ATF CO_2 laser). The undulator length was constrained by the available space on the beamline of the BNL ATF for the 10 period undulator (total length 40cm) and is shown in Fig. 3 - top. The undulator poles are composed of Neodymium-Iron-Boron (NdFeB) magnets which were procured, individually characterized and sorted, then epoxied into tightly toleranced holders. The undulator mechanical design is based on the principles of total access from one side to allow for a Hall probe measurement. The tuning of the magnets occurs from the top (or bottom) allowing flexibility for quick on-the-fly tuning if necessary. The distance of the individual magnets from the center plane is adjusted via the screw that holds the magnet in place. The undulator has variable height endplates, which are readily adaptable to the BNL ATF beamline for alignment. The mounting plate has the capability for fine positional and angular adjustments in the transverse dimensions; the 5-axis degree of freedom stage allows for control of roll.

The undulator fields were characterized using two complimentary methods. First, a Hall probe scan was used to determine some of the magnetic field features directly. The Hall probe scan was performed on the RadiaBeam magnetic measurement station. The first measurement performed is a longitudinal scan of the undulator on-axis. The results of the scan at 33 points/period are shown in Fig. 3 - bottom, where the line represents the simulation performed using Radia, and the dots are the measured field showing good agreement within tolerance.

Second, a pulse wire measurement was performed to measure the effect of the undulator on electron beam transport. For the pulsed-wire measurement, a small current-carrying wire is passed through the magnetically active area of the undulator. The wire displacement is measured by a laser diode detector. In this method, both the first (angle offset) and second (position offset) integral can be measured and tuned out appropriately prior to installation.

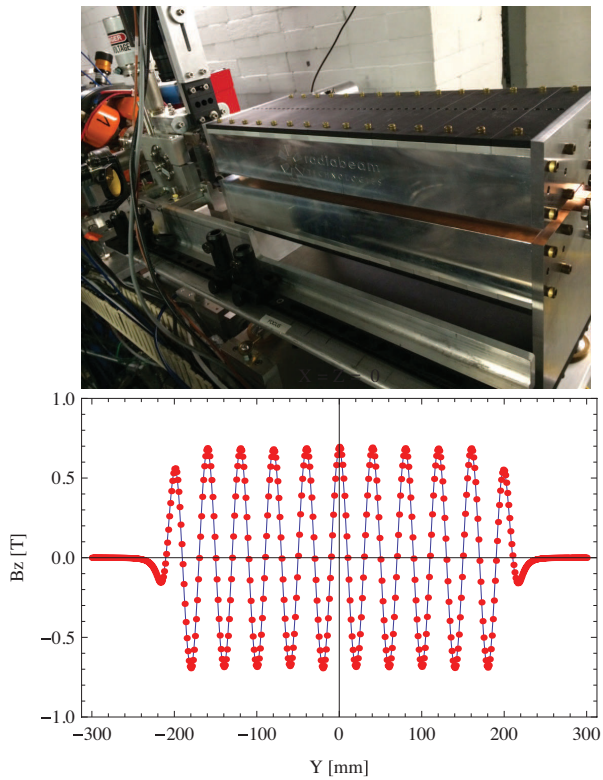

Figure 3: Top: Photograph of the undulator fabricated and installed at the BNL ATF beamline. Bottom: Field profile of undulator as measured on test bench prior to installation.

INITIAL MEASUREMENTS

The challenges of operation at high laser power, necessitate the minimal use of transmissive optics for the purpose of shaping the initial Gaussian laser mode into a higher-order TEM_{10} mode. The generation of the appropriate laser mode is accomplished by a simple interferometer setup. The initial pulse is split in two equal intensity parts and sent through equal length transport arms. The delay between the two arms is controlled by precision micrometer. The two pulses are then recombined at a very shallow angle to produce an interference pattern with the same characteristics as desired. An example of the pattern is shown in Fig. 4 for low-power on the test bench using a pyrocam detector. This interferometric method accurately produces a pulse profile that is characteristically similar to a pure TEM_{10} mode.

Synchronization between the laser pulse and electron beam is critical to observe the interaction. Course synchronization is accomplished by comparing the laser signal on a silicon photodiode and the electron beam at an rf pickup. For further precision, the electron beam transmission through a thin germanium foil with the IR laser is monitored [7]. Ultimately, the observation of the interaction determines the synchronization at the ps time scale.

ISBN 978-3-95450-177-9

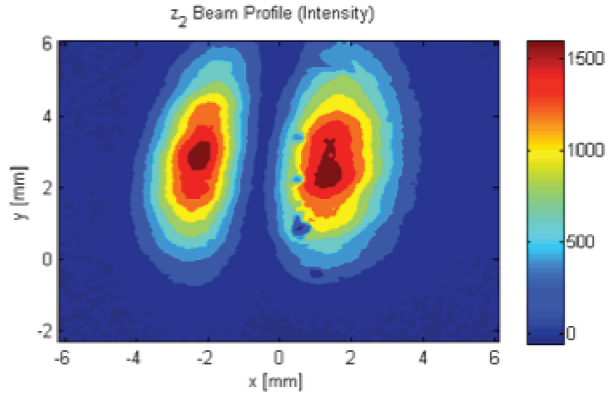

Figure 4: The laser pulse profile of the TEM_{10} mode converter at low power on the test bench.

The first studies employing the undulator and laser interaction were conducted without the deflecting cavity to test the concept feasibility. In this case the main observable is the increase in angular modulation due to increased laser power. The transverse trace space output from the undulator would show an an increase in the projected horizontal beam spread. Fig. 5 shows a qualitative example from simulation for the beam rms transverse size increase in cases of laser driver energy of 10-100GW in the laser modulator section.

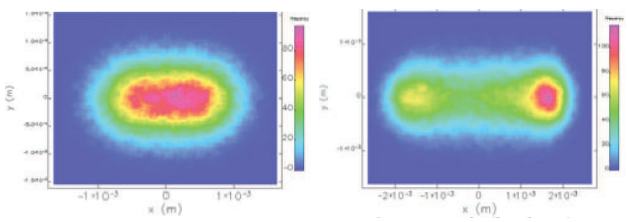

Figure 5: Simulations for the electron beam profile with a 10GW driving laser (left) and 100GW driving laser power (right) shows increase in projected horizontal beam size.

The first beam tests with the interaction at the BNL ATF were conducted prior to installation and commissioning of the x-band transverse deflecting cavity. In these runs, the laser was operated at a power of ~100GW in the higher order mode configuration. The focus of the laser spot was placed at approximately the center of the undulator. The electron beam and laser spatial overlap was determined using beam profile monitors and a co-aligned optical wavelength laser. The electron beam profile was imaged on a screen 1.2 m downstream of the undulator exit. Fig. 6 shows the beam profile on the screen for two cases; first when the laser is off (left), and for the laser powered to 100GW (right). An approximate 25% increase in the horizontal spread (the undulator direction) is seen for the case when the laser is turned on. The increase in the projected rms beam size is an indication of the interaction effect. These results agree with the initial simulations but further work is ongoing on the data analysis to precisely characterize the effect.

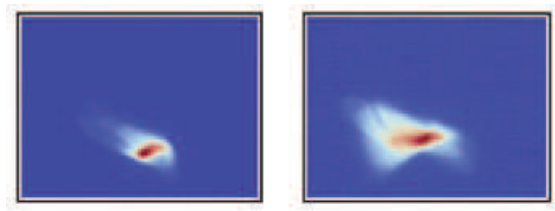

Figure 6: Raw data (uncalibrated) of the electron beam transverse profile at the BNL ATF after traversing through the undulator (left) and when the laser is turned on (right).

CONCLUSIONS

The development of a bunch profile diagnostic with sub-fs resolution has made significant progress in the last year. The initial results without the use of the rf deflecting cavity, presented here, demonstrate the angular modulation of the electron beam from a higher-order laser mode interaction in the resonant undulator. The final results are awaiting the installation and commissioning of the transverse deflecting cavity at the BNL ATF. The complete experiment also has demanding requirements on the electron beam in terms of emittance and energy spread, achievable by the BL ATF. Parallel efforts are also being undertaken to develop analysis tools to directly infer the bunch profile from the screen image for given laser and undulator parameters. In addition, future experiments are being considered to measure the submicron scale microbunching of the beam from an upstream laser modulator using the sub-fs diagnostic. The results are scalable to higher energy beams and optical wavelength lasers and are the subject of continuing and upcoming work.

ACKNOWLEDGMENT

This work is supported by U.S. DOE Grant No. DE-SC0007701.

REFERENCES

[1] R. Lai and A. J. Sievers, Phys. Rev. E 50, R3342 (1994).

[2] R. Akre et al., in Proceedings of the 19th Particle Accelerator Conference, Chicago, Illinois, 2001 (IEEE, Piscataway, NJ, 2001), p. 2353.

[3] G. Andonian, et al., Phys. Rev. ST Accel. and Beams 14, 072802 (2011).

[4] A. Zholents and M. Zolotorev, New J. Phys. 10, 025005 (2008).

[5] M. Fedurin, presented at these proceedings.

[6] M. Borland, Tech. Report Advanced Photon Source LS-287 (2000).

[7] J. Duris, et al., Nat. Comm. 5:4928 (2014).

ISBN 978-3-95450-177-9